Environmental Pollution 230 (2017) 486–494

Contents lists available at ScienceDirect

Environmental Pollution

journal homepage: www.elsevier.com/locate/envpol

Stable isotope analyses of precipitation nitrogen sources in Guiyang, southwestern China☆

Xue-Yan Liu [a, b, c, *, 1], Hong-Wei Xiao [d, e, 1], Hua-Yun Xiao [c, **], Wei Song [a], Xin-Chao Sun [a], Xu-Dong Zheng [a], Cong-Qiang Liu [a, c], Keisuke Koba [b, f]

[a] Institute of Surface-Earth System Science, Tianjin University, Tianjin, 300072, China
[b] Institute of Agriculture, Tokyo University of Agriculture and Technology, Tokyo, 183-8509, Japan
[c] State Key Laboratory of Environmental Geochemistry, Institute of Geochemistry, Chinese Academy of Sciences, Guiyang, 550002, China
[d] Laboratory of Atmospheric Environment, Key Laboratory of Nuclear Resources and Environment (Ministry of Education), East China University of Technology, Nanchang 330013, China
[e] School of Water Resources and Environmental Engineering, East China University of Technology, Nanchang 330013, China
[f] Center for Ecological Research, Kyoto University, Shiga, 520-2113, Japan

ARTICLE INFO

Article history:
Received 30 November 2016
Received in revised form
5 April 2017
Accepted 3 June 2017
Available online 6 July 2017

Keywords:
Stable isotope
Ammonium
Nitrate
Dissolved organic nitrogen
SIAR
Reactive nitrogen emission

ABSTRACT

To constrain sources of anthropogenic nitrogen (N) deposition is critical for effective reduction of reactive N emissions and better evaluation of N deposition effects. This study measured $\delta^{15}N$ signatures of nitrate (NO_3^-), ammonium (NH_4^+) and total dissolved N (TDN) in precipitation at Guiyang, southwestern China and estimated contributions of dominant N sources using a Bayesian isotope mixing model. For NO_3^-, the contribution of non-fossil N oxides (NO_x, mainly from biomass burning (24 ± 12%) and microbial N cycle (26 ± 5%)) equals that of fossil NO_x, to which vehicle exhausts (31 ± 19%) contributed more than coal combustion (19 ± 9%). For NH_4^+, ammonia (NH_3) from volatilization sources (mainly animal wastes (22 ± 12%) and fertilizers (22 ± 10%)) contributed less than NH_3 from combustion sources (mainly biomass burning (17 ± 8%), vehicle exhausts (19 ± 11%) and coal combustions (19 ± 12%)). Dissolved organic N (DON) accounted for 41% in precipitation TDN deposition during the study period. Precipitation DON had higher $\delta^{15}N$ values in cooler months (13.1‰) than in warmer months (−7.0‰), indicating the dominance of primary and secondary ON sources, respectively. These results newly underscored the importance of non-fossil NO_x, fossil NH_3 and organic N in precipitation N inputs of urban environments.

1. Introduction

High production of anthropogenic nitrogen (N) (mainly nitrogen oxides (NO_x), ammonia (NH_3), along with organic N molecules) impairs the air quality in city environments and the chemistry of atmosphere from regional to global scales (Morin et al., 2008; Hastings et al., 2013). The subsequent increases of dissolved N (mainly as nitrate (NO_3^-), ammonium (NH_4^+), dissolved organic N (DON)) in precipitation directly enhance the levels of atmospheric N deposition and influence ecosystem structure and function (Neff et al., 2002; Kendall et al., 2007; Koba et al., 2010). The compositions and deposition levels of NO_3^-, NH_4^+, DON in precipitation are key information for accurately budgeting N deposition and evaluating N pollution (Neff et al., 2002; Cape et al., 2004, 2011). Natural ^{15}N abundance (expressed as $\delta^{15}N$ values) of NO_3^-, NH_4^+ and DON in precipitation provides 'fingerprint' identification of major N sources (Cornell et al., 1995; Knapp et al., 2005; Altieri et al., 2014, 2016). Such information is important for making strategies to reduce airborne N pollution (Alexander et al., 2009; Hastings et al., 2009) and for tracing the biogeochemistry of deposited N in ecosystems (Michalski et al., 2004; Elliott et al., 2007; Altieri et al., 2016).

Precipitation N observations have mostly focused on NO_3^- and NH_4^+, whereas DON has seldom been analyzed extensively or routinely. Actually, DON is an ubiquitous and significant component in total dissolved N (TDN) of precipitation, excluding DON introduces substantial uncertainties in estimating levels and critical

☆ This paper has been recommended for acceptance by Dr. Hageman Kimberly Jill.
* Corresponding author. Institute of Surface-Earth System Science, Tianjin University, Tianjin, 300072, China.
** Corresponding author.
E-mail addresses: liuxueyan@tju.edu.cn (X.-Y. Liu), xiaohuayun@vip.skleg.cn (H.-Y. Xiao).
[1] These authors contributed equally to this work.

http://dx.doi.org/10.1016/j.envpol.2017.06.010
0269-7491/

loads of N deposition (Cornell et al., 2003; Aneja et al., 2011; Cornell, 2011). To analyze precipitation DON concentrations and deposition levels in polluted environments is necessary for understanding the provenance and importance of DON in elevated N deposition (Carrillo et al., 2002; Cape et al., 2004). Atmospheric DON can originate from terrestrial and oceanic, natural and anthropogenic, primary and secondary sources (Cornell et al., 2001; Neff et al., 2002). Components and sources of terrestrial DON in the atmosphere are more diverse and complex than those of oceanic ones (Cornell et al., 1995; Russell et al., 1998). Natural DON can be derived from sea spray droplets and plant pollen (Prospero et al., 1996), while anthropogenic DON includes primary emissions directly from fossil-fuel and biomass combustion, fertilizers and secondary production from inorganic N species via the reaction with non-N-containing organic compounds (Chang and Novakov, 1975; Prospero et al., 1996; Cornell et al., 2001; Neff et al., 2002). For example, the transformations of NH_3 to ON have been clearly verified in experimental studies (Na et al., 2007; Nozière et al., 2009), which is a potential source of ON in atmospheric dry and wet deposition. The $\delta^{15}N$ values of DON in urban precipitation provide source information of atmospheric DON under N-polluted environments. However, a robust separation of detailed DON components for direct $\delta^{15}N$ analysis of remain difficult (Cornell et al., 1995; Feuerstein et al., 1997; Knapp et al., 2005). Using the ultraviolet photo-oxidation of DON to NO_3^- and subsequent reduction of NO_3^- to N_2 (Rendell et al., 1993), Cornell et al. (1995) first measured $\delta^{15}N$ values of DON in rain and snow samples, showing a wide distribution of −7.3‰ to +7.3‰. By comparing with $\delta^{15}N$ values of potential sources, Cornell et al. (1995) attributed the negative $\delta^{15}N$ values of rain DON at marine sites to anthropogenic NO_x and NH_3 sources or products of marine denitrification, while positive values at continental sites to primary sources from soil and vegetation. Using the same method, Russell et al. (1998) observed more positive $\delta^{15}N$ values of precipitation DON (−0.5‰ to +14.7‰) in Chesapeake Bay region, speculating common origins between DON and NO_3^- from fossil-fuel combustions. However, both studies (Cornell et al., 1995; Russell et al., 1998) emphasized that the direct processing using UV light irradiation may underestimate the contribution of DON in N deposition, especially causing worse precision in samples with high inorganic N and low DON. Alternatively, $\delta^{15}N$ values of DON can be calculated through a $\delta^{15}N$ mass balance equation between TDN and dissolved inorganic N (DIN) plus DON (TDN = DON + DIN), which has been widely performed on water and soil samples (Koba et al., 2010, 2012; Altieri et al., 2013, 2016). Using this method, a wider $\delta^{15}N$ distribution of aerosol DON (+13.2 ± 18.6‰) was recently observed on the island of Bermuda in the western North Atlantic Ocean (Altieri et al., 2016).

Precipitation $\delta^{15}N$ studies were mostly conducted on NO_3^- and NH_4^+ since 1950s (Hoering, 1957). However, precise analyses of NO_3^- and NH_4^+ sources in precipitation have been always prevented from the fact that each of these ions in the atmosphere is derived from a mixture of multiple emission sources and is a product of complicate physical and chemical processing on the emission sources. **Therefore, there are two important conditions or assumptions for that $\delta^{15}N$ values of precipitation NH_4^+ or NO_3^- can differentiate contributions of major emissions sources**.

First, $\delta^{15}N$ values of dominant NH_3 or NO_x emissions are distinct and well characterized. In the urban environments, dominant emission sources for precipitation NO_3^- include ^{15}N-enriched NO_x from coal combustion and biomass burning, ^{15}N-depleted NO_x from vehicle exhausts, microbial N cycle of soil and animal/urban wastes (Table S1). For precipitation NH_4^+ sources, both volatilization NH_3 (mainly from animal wastes and fertilizers) and fossil NH_3 sources (mainly from coal combustion and vehicle exhausts) showed negative $\delta^{15}N$ values (Table S1). A potential origin of ^{15}N-enriched NH_3 is biomass burning, whose $\delta^{15}N$ value was estimated by that of aerosol NH_4^+ (12.1‰) in winter at Yurihonjo, Japan (Kawashima and Kurahashi, 2011) though direct measurements are still unavailable. Obviously, $\delta^{15}N$ values of NH_3 and NO_x emissions are still very limited and have substantial variabilities. Extant studies showed that NH_3 volatilization from animal wastes and fertilizers are temperature-dependent and can cause ^{15}N enrichments in both remaining NH_4^+ thus later NH_3 emissions over time (Mariappan et al., 2009). In the laboratory study of Li and Wang (2008), the $\delta^{15}N$ values of NO from microbial N cycle increased gradually over the time of soil incubation. $\delta^{15}N$ values of NO_x from coal combustion were influenced by the use of NO_x scrubbing technology, with significantly higher $\delta^{15}N$ values in NO_x undergone catalytic NO_x reduction (Felix et al., 2012). The $\delta^{15}N$ variations of NO_x from vehicle exhausts showed a Rayleigh pattern with the NO_x emissions, which is linked to engine warming-up and by extension local commute characteristics (Walters et al., 2015). Recently, $\delta^{15}N$ of NO_x from biomass burning was found to be a function of biomass $\delta^{15}N$ values (Fibiger and Hastings, 2016). Walters et al. (2016) observed diurnal and seasonal variations in $\delta^{15}N$ of NO_x, which might be influenced by internal isotope exchange between NO and NO_2, in turn is dependent on meteorological factors such as temperature, solar radiation, and other oxidant constituents (e.g., OH, O_3, VOC). Accordingly, it remains a challenge to well characterize and localize source $\delta^{15}N$ values, and to assign source $\delta^{15}N$ values for precipitation $\delta^{15}N$ analysis more specifically.

Second, precipitation scavenges both gaseous and particulate N species efficiently because researchers have revealed isotopic fractionations associated with the formations of NO_3^- and NH_4^+ in atmospheric particulates, then differing rainout efficiency between gaseous and particulate N species would change the initial $\delta^{15}N$ values of emission sources in precipitation (Heaton, 1987; Heaton et al., 1997; Altieri et al., 2014). In controlled experiments, large ^{15}N enrichment of particulate NH_4^+ due to the NH_3 (*g*) ↔ NH_4^+ (*p*) equilibrium was found (+33‰; Heaton et al., 1997), resulting in $\delta^{15}N$ values of particulate NH_4^+ higher than the remaining NH_3. For NO_3^-, NO is the major form of most initial NO_x emissions. However, the measurable NO in the atmosphere is a mixture of NO emissions and NO_2 photolysis-derived NO. Upon entering the atmosphere, most of NO emissions would be rapidly oxidized (thus NO has much shorter life time) to NO_2 then finally to NO_3^-. Isotope exchange equilibrium would occur during the NO-NO_2 cycle. In simulated experiments with very 'beneficial' conditions (e.g., closed systems, no adequate oxidants, long mixing time to achieve an equilibrium exchange) (Monse et al., 1969; Freyer et al., 1993; Heaton et al., 1997; Walters et al., 2016), N isotope equilibrium exchange fractionations were observed (>34‰; depending on the experimental conditions), making ^{15}N enrichment in more oxidized forms. Moreover, the kinetic fractionation of gaseous NO_2 oxidation to gaseous HNO_3 was simulated as −3‰ (Freyer, 1991). The equilibrium fractionation for gaseous HNO_3 and NH_4NO_3 particles was determined as +21‰ in the laboratory (Heaton et al., 1997). Differently, in the study of Geng et al. (2014), the $\delta^{15}N$ differences (−8.5 ± 2.5‰) between snow NO_3^- and gaseous HNO_3 during photolysis (Erbland et al., 2012) were assumed as the equilibrium fractionations between gaseous HNO_3 and particulate/aqueous NO_3^-. In general, these processes would result in higher $\delta^{15}N$ in particulate NO_3^- than the initial NO_x sources.

In the 'real' atmosphere systems, however, isotopic fractionations associated with NO_3^- and NH_4^+ formations have been poorly known. Researchers often assumed efficient scavenging of both gaseous and particulate N species into precipitation thus no substantial $\delta^{15}N$ difference between initial N emissions and precipitation N. For examples, NO_x from coal combustion and vehicle exhausts were directly attributed to be the dominant sources for positive and negative $\delta^{15}N$ values of precipitation NO_3^- observed in urban environments, respectively (Xiao and Liu, 2002; Fang et al., 2011; Felix et al., 2013; Walters et al., 2015). NH_3 from domestic wastes and sewage was inferred to be the dominant contributor to negative $\delta^{15}N$ values of precipitation NH_4^+ in major cities of China (Xiao et al., 2012; Xiao and Liu, 2002, 2011). In this work, to characterize the importance of DON and to determine contributions of major inorganic N sources in atmospheric N deposition, we measured the deposition levels and $\delta^{15}N$ values of NO_3^-, NH_4^+ and DON in precipitation across cooler and warmer months at Guiyang urban, southwestern China. By considering isotopic fractionations associated with NO_3^- and NH_4^+ formations (Heaton et al., 1997; Altieri et al., 2014; Walters et al., 2015), we inferred whether $\delta^{15}N$ values have been substantially modified from emissions to precipitation or not. Then a Bayesian isotope mixing model (SIAR, Stable Isotope Analysis in R; details in Supporting Information (SI)) was used to quantify contributions of dominant N sources in precipitation NO_3^- and NH_4^+, respectively. Due to insufficient knowledge of origins and components of atmospheric DON, an attribution of specific sources to precipitation DON is difficult until now. However, the depletion or enrichment of ^{15}N in precipitation DON may provide useful evidences on the relative importance of primary and secondary ON sources (Cornell et al., 1995; Russell et al., 1998; Altieri et al., 2016).

2. Materials and methods

2.1. Study site and sample collection

Guiyang is one of the major cities suffering from severe acid deposition in SW China since the 1980s (Xiao et al., 2012; Xiao and Liu, 2002). The sampling site was located in the Institute of Geochemistry, Chinese Academy of Sciences (26°35′N, 106°43′E), which is a typical urban site of Guiyang (see detailed description in Xiao and Liu (2002)). The $\delta^{15}N$ values of NO_3^- and NH_4^+ in precipitation at this site were first measured in rain samples in July of 2001 (Xiao and Liu, 2002). To better characterize anthropogenic N in local N deposition, a year-round collection of precipitation was conducted at the same site from Oct-2008 to Sep-2009 (See details of precipitation collection in Xiao et al. (2012). In this study, forty-four daily-integrated samples were collected from the cooler (3.3 ± 1.8 °C) months (Dec-2008 to Mar-2009; $n = 17$) and warmer (18.1 ± 3.4 °C) months (Apr-Sept, 2009; $n = 27$) (Fig. 1a). The annual rainfall at Guiyang (1107 mm in 2009) has a distinct seasonal pattern, with 70% falling during the warmer and rainy months (Apr-Sept) and much less precipitation in cooler months (Oct-Mar).

2.2. Chemical analyses

Upon collection, precipitation samples were filtered and immediately frozen (at −20 °C). Part of the filtered samples were brought to Tokyo University of Agriculture and Technology (Japan), the other part of samples was mainly used for $\delta^{15}N$ analysis of NH_4^+ (Xiao et al., 2012). The concentrations of NH_4^+ were determined by spectrophotometry after treatment with Nessler's reagent (Xiao et al., 2012). The concentrations of NO_3^- and TDN were determined by ion chromatography (IC) (Dionex DX-120, Osaka, Japan), the same as that described in Li et al. (2012). The TDN was digested to NO_3^- using alkaline persulfate digestion and measured as NO_3^- on IC. The concentrations of DON were calculated as the differences between TDN and DIN. Nitrate-N standards (at concentrations of 20, 50, 100, 250, 500 μmol-N L^{-1}, respectively) were run with samples in the whole process of digestion. The NO_3^- concentrations after oxidation were found 1%–4% (on average 2%) higher than initial concentrations, suggesting no N loss during the treatment. We used three standards of amino acids (alanine, histidine and glycine) (at 10, 20, 50, 100, 250, 500 μmol-N L^{-1}, respectively) to examine the recovery in the oxidation process. The efficiency of oxidation was found to be relatively lower (88%) when concentrations of DON were higher than 500 μmol-N L^{-1}, below which the oxidation efficiencies were on average 96%, 100% and 99% for alanine, histidine and glycine, respectively. Thus, the concentrations of DON in the samples with concentrations higher than 500 μmol-N L^{-1} might have been underestimated. However, the highest concentration of precipitation DON in this study was 406 μmol-N L^{-1}, suggesting that the oxidation process was completed overall and DON concentration measurements were not significantly underestimated.

The $\delta^{15}N$ ratios of NO_3^- ($\delta^{15}N_{NO3-}$) were measured using the denitrifier method, detailed procedures of sample pretreatment and analyses were the same as those in Fang et al. (2011). The average standard deviation for replicate analyses of an individual sample was ±0.2‰ (SD) for $\delta^{15}N$ of NO_3^-. In this study, four precipitation samples contained NO_2^- higher than 0.07 mg-N L^{-1} (5 μmol-N L^{-1}), but accounting for 1.6%–4.1% of total NO_3-N (NO_3^- plus NO_2^-) in corresponding samples. We expect insignificant analytical artifact resulting from the presence of NO_2^-, so that we refer to the sum of NO_2^- plus NO_3^- as NO_3^- in these samples. The $\delta^{15}N$ of TDN ($\delta^{15}N_{TDN}$) was determined by analyzing the persulfate-digested samples using the same denitrifier method as that used for NO_3^- (Koba et al., 2010). Three isotopic standards (alanine, glycine and histidine) dissolved in deionized water were used for calibrating the $\delta^{15}N$ of TDN. We also analyzed several TDN samples for the deionized water to correct for the effect of the N blank from chemicals. The average standard deviation for replicate analyses of $\delta^{15}N_{TDN}$ in an individual sample was ±0.3‰. The $\delta^{15}N$ values of NH_4^+ ($\delta^{15}N_{NH4+}$) were measured using the diffusion method as described in Xiao et al. (2012). The $\delta^{15}N$ values of DON ($\delta^{15}N_{DON}$) were calculated using the isotope mass balance equation:

$$\delta^{15}N_{DON}\ (‰) = (\delta^{15}N_{TDN} \times [TDN] - \delta^{15}N_{NO3-} \times [NO_3^-] - \delta^{15}N_{NH4+} \times [NH_4^+]) / [DON].$$

The propagated experimental error in calculating $\delta^{15}N_{DON}$ values was estimated using a Monte Carlo method as described by Koba et al. (2012) and Knapp et al. (2010). Assuming that analytical standard deviations (from replicate measurements) were ±3 μg-N L^{-1} for $[NH_4^+]$ and $[NO_3^-]$, ±4 μg-N L^{-1} for [TDN], ±0.5‰ for $\delta^{15}N_{NH4+}$, ±0.2‰ for $\delta^{15}N_{NO3-}$ and ±0.3‰ for $\delta^{15}N_{TDN}$, and using average concentrations and $\delta^{15}N$ values, the estimated analytical error averaged ±6.2 μg-N L^{-1} for [DON] and ±1.3‰ for $\delta^{15}N_{DON}$.

In our previous studies, arithmetic mean values of $\delta^{15}N_{NO3-}$ and $\delta^{15}N_{TDN}$ of precipitation samples in the study period were used for discussing $\delta^{15}N$ records in moss bio-indicator (Liu et al., 2012). Using the monthly mean values of $\delta^{15}N_{NH4+}$, $\delta^{15}N_{NO3-}$ and $\delta^{15}N_{TDN}$, the monthly $\delta^{15}N_{DON}$ values were calculated for discussing their contributions to moss N (Liu et al., 2013). In this study, the $\delta^{15}N_{DON}$ values were re-calculated using $\delta^{15}N_{NH4+}$, $\delta^{15}N_{NO3-}$ and $\delta^{15}N_{TDN}$ values in each sample, aiming at quantifying NO_3^- and NH_4^+ sources, and characterizing the importance of DON in precipitation N deposition.

2.3. Statistical analyses

Statistical analyses were conducted using SigmaPlot software 11.0. An α level of 0.05 was inferred as indicating significance. One-way ANOVA was performed for concentrations and isotopic values of precipitation N species in order to identify the differences between cooler and warmer seasons. Two-way ANOVA was used to

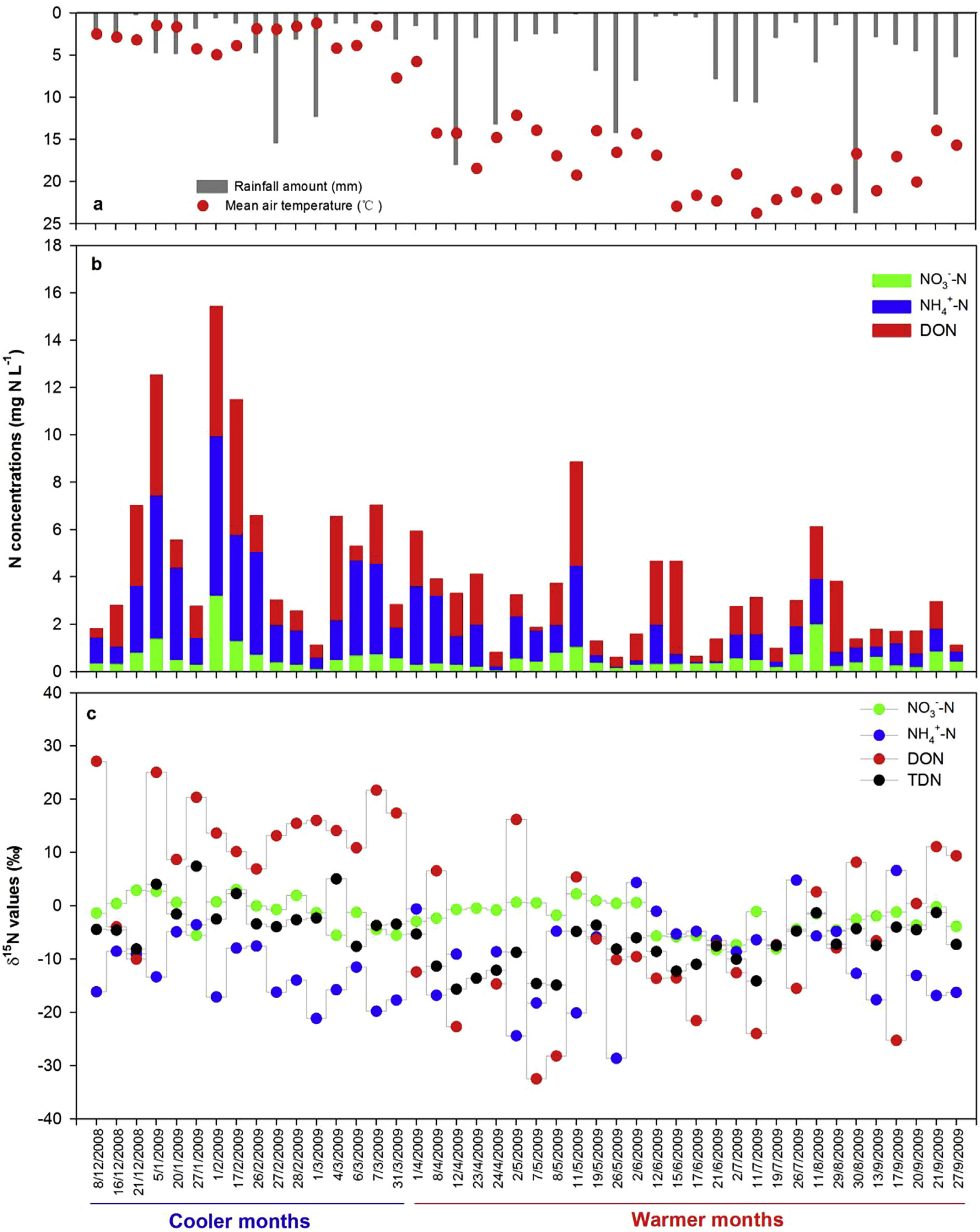

Fig. 1. Daily precipitation amount and mean air temperature (a), concentrations (b) and $\delta^{15}N$ values (c) of NO_3^--N, NH_4^+-N and DON in daily-integrated precipitation collected on 44 days from Dec-2008 to Sept-2009 at Guiyang city, China.

identify the significance between samples for the investigated variables across the study period. Spearman's correlation coefficient was used to assess correlation among meteorological data and concentration or isotopic data across the study period. Statistically significant difference was set at *P* values < 0.05 unless otherwise stated.

3. Results and discussion

3.1. Precipitation N deposition

Concentrations of dissolved N in precipitation generally decreased with the increase of precipitation amount (Table S2; Fig. 1ab). The precipitation TDN deposition was estimated as 24.8 kg N ha^{-1} across the study period (Fig. 2a), in which NO_3^--N, NH_4^+-N and DON accounted for 17%, 42% and 41%, respectively (Fig. 2b). Using the annual precipitation amount, the annual level of DON deposition at Guiyang city can be estimated as 12.6 kg N ha^{-1} yr^{-1}, which was within the ranges of annual DON deposition reported at other urban/suburban sites of China (from 3 kg N ha^{-1} yr^{-1} to 18 kg N ha^{-1} yr^{-1}; accounting for 12%–36% of TDN) (Li et al., 2012). In China, the levels of DON deposition varied widely between 0.4 kg N ha^{-1} yr^{-1} to 26 kg N ha^{-1} yr^{-1} and accounted for 2%–78% in TDN deposition at rural, remote, marine and forested sites (Shi et al., 2010; Zhang et al., 2008, 2012). Precipitation DIN at Guiyang city was dominated by NH_4^+-N (Table S3). The NH_4^+-N:NO_3-N values averaged 5.0 in 2001 (Xiao et al., 2012) and decreased to 2.4 in 2009, which fell in the lower range of NH_4^+-N:NO_3-N values (1.5–22) among major cities of southern China (Xiao and Liu, 2011).

3.2. Major sources of NO_3^- in precipitation

Precipitation $\delta^{15}N_{NO3-}$ ranged between −8.3‰ and +3.0‰ (mean = −1.9 ± 3.0‰; Fig. 1c; Table S4). There was no clear relationship between precipitation amount and $\delta^{15}N$ values of dissolved N (Table S2), suggesting a weak influence of precipitation amount on variations of precipitation $\delta^{15}N$. The dissolved N in precipitation was incorporated through the dissolution ("washout") and scavenging of gaseous N precursors and particulate N by ascending water vapor and by subsequently falling condensed water (precipitation). As reviewed in the Introduction, equilibrium isotope fractionations associated with the NO-NO_2 cycle potentially cause higher $\delta^{15}N$ signatures in NO_2 that is subsequently oxidized to NO_3^- in particulates (Freyer et al., 1993; Heaton et al., 1997; Walters et al., 2016). In that case, $\delta^{15}N$ signatures of precipitation NO_3^- would differ from those of NO_x emissions unless precipitation can integrate both gaseous and particulate N species. In our study, if precipitation NO_3^- was derived from NO_2 that has been enriched in ^{15}N due to the NO-NO_2 cycle, the expected $\delta^{15}N$ values of initial NO_x emissions would be −42.3‰ to −31.0‰ (by considering the least isotopic exchange equilibrium of 34‰), which appeared not explainable by $\delta^{15}N$ values of major NO_x emission sources (−30.3‰ to +12.5‰ on average; Table S1). Accordingly, we assumed negligible difference in $\delta^{15}N$ values between NO_x emission sources and precipitation NO_3^- in this study. A similar assumption has also been made for the incorporation of gaseous and particulate N into precipitation (Baker et al., 2007; Elliott et al., 2009; Morin et al., 2009).

Using $\delta^{15}N$ values of NO_x sources (Table S1), the fractional contributions of major NO_x sources to precipitation NO_3^- were estimated by the SIAR model (Fig. S1 and Fig. 3 for analytical results of each month and period, respectively; see methodological details in SI). It should be noted that NO_x from microbial N cycle includes the sum of NO_x from natural soils and agricultural soils, aquatic ecosystems, urban sewage, and animal wastes in both urban and rural areas, etc (assuming that NO_x from these sources did not differ in $\delta^{15}N$ values). The modeling results showed that NO_x from biomass burning, NO_x from coal combustion, NO_x from microbial N cycle and NO_x from vehicle exhausts accounted for 24 ± 12%, 19 ± 9%, 26 ± 5% and 31 ± 11% in precipitation NO_3^-, respectively

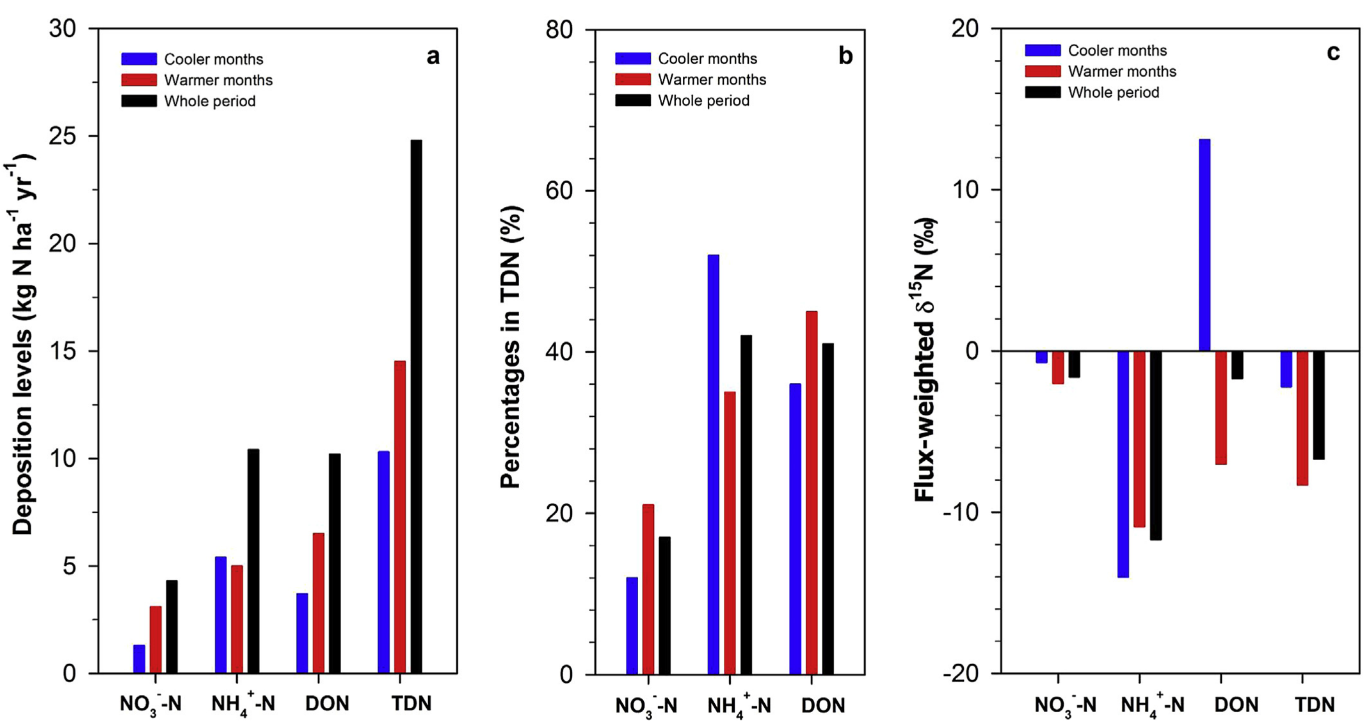

Fig. 2. The deposition levels (a), percentages in TDN (b) and flux-weighted $\delta^{15}N$ values (c) of NO_3^--N, NH_4^+-N and DON in precipitation across the cooler months (Dec-2008 to Mar-2009), warmer months (Apr-2009 to Sept-2009) and the whole period (Dec-2008 to Sept-2009) at Guiyang city, China.

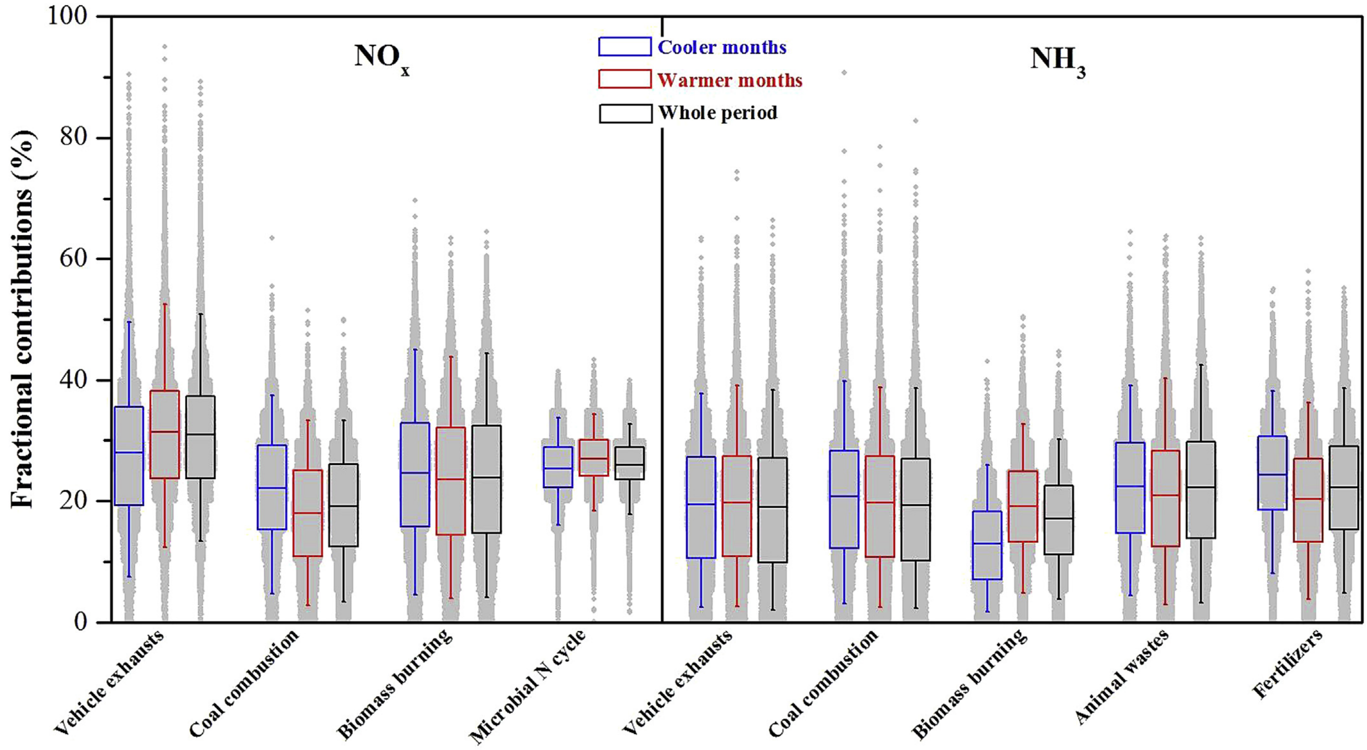

Fig. 3. The fractional contributions of dominant NO_x sources to NO_3^--N, dominant NH_3 sources to NH_4^+-N in precipitation across the cooler months (Dec-2008 to Mar-2009), warmer months (Apr-2009 to Sept-2009) and the whole period (Dec-2008 to Sept-2009) at Guiyang city, China. Grey points are percentage data ($n = 10000$) output from the SIAR model. Each box encompasses the 25th–75th percentiles, whiskers are the 5th and 95th percentiles. The line in each box marks the mean fractional contribution.

(Fig. 3). These results demonstrated the apparent contributions of non-fossil NO_x to NO_3^--N in urban precipitation. Biomass burning, as a non-point and ^{15}N-enriched NO_x source (Hastings et al., 2009; Morin et al., 2009; Agnihotri et al., 2011; Felix et al., 2014), as well as NO_x from microbial N cycle, substantially influenced $\delta^{15}N_{NO3-}$ signatures in urban precipitation. Compared with the $\delta^{15}N_{NO3-}$ values of precipitation collected in 2001 (ca. +2.0 ± 4.4‰) (Xiao and Liu, 2002), precipitation $\delta^{15}N_{NO3-}$ in 2009 (ca. −1.9 ± 3.0‰; Table S4) decreased by 3.9‰ on average. Before this study, decreased $\delta^{15}N_{NO3-}$ has been attributed to enhanced NO_x emission from vehicle exhausts in Guiyang city (Xiao and Liu, 2002; Li et al., 2012; Liu et al., 2012; Xiao et al., 2013). According to analysis of the SIAR model in this work, however, we found that fractional contributions of corresponding NO_x sources to precipitation NO_3^- did not differ significantly between 2001 and 2008–2009 (Fig. S1e). Although the mean contributions did decrease by 9% for NO_x from coal combustion and increase by 6% and 6%, respectively for NO_x from microbial N cycle and vehicle exhausts in 2009, it remains unresolved whether changes of non-fossil or fossil NO_x emissions are more important in driving precipitation $\delta^{15}N_{NO3-}$ decreases in Guiyang city.

3.3. Major sources of NH_4^+ in precipitation

The range and mean value of $\delta^{15}N_{NH4+}$ in precipitation are −28.7‰ to +6.6‰ (Fig. 1c) and −10.6 ± 7.7‰ (Table S4), respectively. These values assembled those reported for precipitation NH_4^+ presumably dominated by volatilization NH_3 sources (e.g., Freyer, 1978; Heaton et al., 1997; Zhang et al., 2008; Koba et al., 2012; Altieri et al., 2014) (Table S1). In Guiyang city, the ^{15}N depletion of precipitation NH_4^+ has also been attributed to the NH_3 emissions from domestic wastes and sewage (Xiao and Liu, 2002; Liu et al., 2012; Xiao et al., 2013). However, the importance of other NH_3 sources (particularly fossil-derived NH_3) to precipitation NH_4^+ remains unclear. Moreover, as introduced in the Introduction, precipitation NH_4^+ was scavenged from both NH_3 and particulate NH_4^+, the isotopic fractionations associated with NH_3 (*g*) ↔ NH_4^+ (*p*) equilibrium should be justified for measuring contributions of initial NH_3 emissions based on precipitation $\delta^{15}N_{NH4+}$ signatures.

In our study, precipitation NH_4^+ showed δ^{15}N values of −28.7‰ to +6.6‰ (−10.6 ± 7.7‰), if these values have been elevated due to isotopic equilibrium fractionations (+33‰; Heaton et al., 1997), the expected δ^{15}N values of initial NH_3 emissions would range between −61.7‰ and −26.4‰, which appeared not explainable by δ^{15}N values of major NH_3 sources (−27‰ to +12‰ on average; Table S1). Accordingly, we assumed negligible difference in δ^{15}N values between emission NH_3 sources and precipitation NH_4^+ in this study. Further, we calculated the proportional contributions of six dominant NH_3 sources to precipitation NH_4^+ (Fig. S2 and Fig. 3 for results of each month and period data analyses, respectively; see methodological details in SI). We found that precipitation NH_4^+ in Guiyang city was originated more from fossil fuel-derived NH_3 emissions (19 ± 12% for NH_3 from coal combustion, 19 ± 11% for NH_3 from vehicle exhausts) and biomass burning (17 ± 8%) than from volatilization NH_3 emissions (22 ± 12% for NH_3 from animal wastes, 22 ± 10% for NH_3 from fertilizers) (Fig. 3). Accordingly, the NH_3 emissions from domestic wastes and sewage might be overestimated in our previous studies (Xiao and Liu, 2002; Liu et al., 2012; Xiao et al., 2013). Combustion NH_3 sources especially that from fossil fuels substantially contributed to the observed ^{15}N depletion of precipitation NH_4^+ in the urban environment, which should be emphasized in source measurement of anthropogenic NH_4^+ deposition.

3.4. $\delta^{15}N$ signatures of DON in precipitation

Precipitation $\delta^{15}N_{TDN}$ showed a range of −15.7‰ to +7.4‰ (Fig. 1c). The depletion of ^{15}N in precipitation TDN (−6.0 ± 5.2‰; Table S4) suggested that elevated/anthropogenic N deposition potentially influenced ^{15}N abundance of N-limiting ecosystems in the study area. Precipitation $\delta^{15}N_{DON}$ showed a range of −32.5‰ to +26.6‰ (Fig. 1c), which is much wider than that (−7.3‰ to +15.0‰) reported for non-urban sites by Cornell et al. (1995) and Russell et al. (1998). Unexpectedly, precipitation $\delta^{15}N_{DON}$ showed significantly higher values in cooler months than in warmer months (Table S4; Fig. 1c). The flux-weighted $\delta^{15}N_{DON}$ value was −7.0‰ in warmer months and +13.1‰ in cooler months (Fig. 2c). A wider $\delta^{15}N$ range of precipitation DON indicated heterogeneous and complex DON origins, especially in continental and urban precipitation (Cornell et al., 1995; Russell et al., 1998; Cape et al., 2011; Altieri et al., 2016). Using the air mass back trajectories, Altieri et al. (2016) reported that marine and continental DON sources had mean $\delta^{15}N$ values of −0.2 ± 4.6‰ and +2.6 ± 9.2‰, respectively. More variable $\delta^{15}N$ signatures (+13.2 ± 18.6‰) were observed in aerosols on the island of Bermuda in the western North Atlantic Ocean, but no difference between warmer (+10.5 ± 4.9‰) and cooler seasons (+15.9 ± 26.3‰) was found (Altieri et al., 2016).

In our study, positive precipitation $\delta^{15}N_{DON}$ values reflected the dominance of primary DON sources, most possibly from biomass and fossil-fuel combustions (Cornell et al., 1995). Previously, organic N (ON) emitted from the burning of different types of biomass (used as fuel wood, crop residues) and coal (used for cooking and energy production activities) showed $\delta^{15}N$ values of +5‰ to +21‰ (+12 ± 5‰) (Morin et al., 2009). Because marine DON sources would be not very depleted in ^{15}N (Cornell et al., 1995; Russell et al., 1998; Altieri et al., 2016), the negative precipitation $\delta^{15}N_{DON}$ in warmer months at Guiyang city suggested little contribution from marine ON sources, which was supported by the air mass backward trajectories (Fig. S3). We inferred that negative precipitation $\delta^{15}N_{DON}$ was influenced by secondary DON sources formed by the reaction of ^{15}N-depleted inorganic N with organic molecules (Atkinson, 2013; Na et al., 2007; Nozière et al., 2009). First, there were opposite seasonal patterns between $\delta^{15}N_{NH4+}$ and $\delta^{15}N_{DON}$ (Table S4; Fig. 4), the ^{15}N depletion in NH_3 as well ^{15}N discrimination during NH_3 transformation to organic molecules might explain the observed ^{15}N depletion of precipitation DON in warmer months. Second, higher precipitation amount should have caused NH_4^+-N deposition higher in warmer months higher than in cooler months. In contrast, NH_4^+-N deposition in warmer months was similar to that in cooler months, while DON deposition in warmer months was significantly higher than that in cooler months (Fig. 2ab).

4. Remarks

The analyses of precipitation $\delta^{15}N$ values with a Bayesian isotope mixing model (SIAR) provide a quantitative solution to re-examine contributions of major N sources to precipitation N inputs in urban environments. In the study city, non-fossil NO_x (mainly from biomass burning and microbial N cycle) and fossil NO_x equally contributed to the NO_3^- in the urban precipitation, and vehicle exhausts contributed more NO_x than coal combustion. The contributions of NH_3 from combustion sources (mainly biomass burning, vehicle exhausts and coal combustions) were found higher than that of NH_3 from volatilization sources (mainly animal wastes and fertilizers). Moreover, DON is an important fraction in urban N deposition via precipitation. Distinct $\delta^{15}N_{DON}$ values between cooler months and warmer months indicated the dominance of primary and secondary ON sources, respectively. These information highlighted the importance of non-fossil NO_x, fossil NH_3 and organic N in precipitation N of urban environments, which is useful for effective reduction of reactive N emissions and better evaluation of N deposition impacts.

However, it should be noted that the source $\delta^{15}N$ values can vary temporally and highly depend on the local conditions of emissions, thus localized source $\delta^{15}N$ data should be measured specifically for more accurate analyses of N deposition sources based on $\delta^{15}N$. Moreover, isotopic fractionations associated with the formations of dissolved N in the atmosphere have not properly considered into the source measurements of this work, partly because of very limited knowledge on *in situ* fractionation mechanisms. Extant fractionation information obtained in laboratory studies cannot be always applicable or predictable for precipitation $\delta^{15}N$, which may

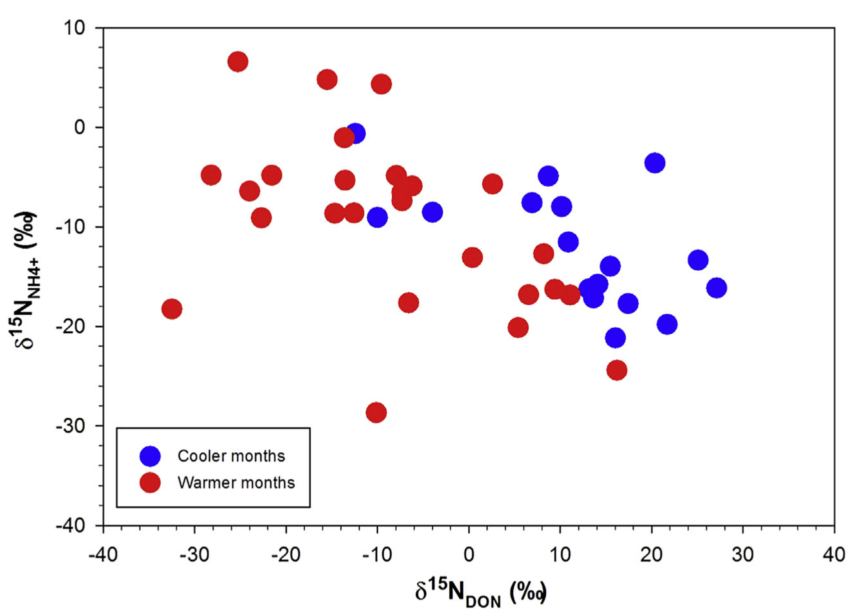

Fig. 4. Correlations between $\delta^{15}N_{DON}$ and $\delta^{15}N_{NH4+}$ ($y = -0.25x - 10.72$, $R^2 = 0.24$, $P < 0.001$) in precipitation at Guiyang city, China.

substantially integrate $\delta^{15}N$ signals of gaseous and particulate N species. But it should be stressed that NO has a much lower solubility relative to NO_2 and NH_3, and it is impossible to have no difference in washout efficiency between gaseous N and particulate N species. These can drive precipitation $\delta^{15}N$ variations thus constitute potential uncertainties to be clarified in future works..

Acknowledgements

This work was supported by the National Key Research and Development Program of China (2017YFC0210100), (2016YFA0600802), the National Natural Science Foundation of China (Nos. 41273026, 41425014, 41522301, 41603007), the Sumitomo Foundation together with NEXT Program (GS008) from Japan Society for the Promotion of Science (JSPS), a grant-in-aid for scientific research from JSPS (No. P09316), the 11st Recruitment Program of Global Experts (the Thousand Talents Plan) for Young Professionals granted by the central budget of China, and Youth Innovation Promotion Association of CAS (No. 2015327).

Appendix A. Supplementary data

Supplementary data related to this article can be found at http://dx.doi.org/10.1016/j.envpol.2017.06.010.

References

Agnihotri, R., Mandal, T.K., Karapurkar, S.G., Naja, M., Gadi, R., Ahammmed, Y.N., Kumar, A., Saud, T., Saxena, M., 2011. Stable carbon and nitrogen isotopic composition of bulk aerosols over India and northern Indian Ocean. Atmos. Environ. 45, 2828–2835.

Alexander, B., Hastings, M.G., Allman, D.J., Dachs, J., Thornton, J.A., Kunasek, S.A., 2009. Quantifying atmospheric nitrate formation pathways based on a global model of the oxygen isotopic composition ($\Delta^{17}O$) of atmospheric nitrate. Atmos. Chem. Phys. 9, 5043–5056.

Altieri, K.E., Fawcett, S.E., Peters, A.J., Sigman, D.M., Hastings, M.G., 2016. Marine biogenic source of atmospheric organic nitrogen in the subtropical north atlantic. Proc. Natl. Acad. Sci. U. S. A. 113 (4), 925–930.

Altieri, K.E., Hastings, M.G., Gobel, A.R., Peters, A.J., Sigman, D.M., 2013. Isotopic composition of rainwater nitrate at Bermuda: the influence of air mass source and chemistry in the marine boundary layer. J. Geophys Res. 118 (D19), 11304–11316.

Altieri, K.E., Hastings, M.G., Peters, A.J., Oleynik, S., Sigman, D.M., 2014. Isotopic evidence for a marine ammonium source in rainwater at Bermuda. Glob. Biogeochem. Cy 28 (10), 1066–1080.

Aneja, V.P., Roelle, P.A., Murray, G.C., Southerland, J., Erisman, J.W., Flower, D., Asman, W.A.H., Patni, N., 2011. Atmospheric nitrogen compounds II: emissions, transport, transformation, deposition and assessment. Atmos. Environ. 35, 1903–1911.

Atkinson, R., 2013. Atmospheric chemistry of VOCs and NO_x. Atmos. Environ. 34, 2063–2101.

Baker, A.R., Weston, K., Kelly, S.D., Voss, M., Streu, P., Cape, J.N., 2007. Dry and wet deposition of nutrients from the tropical Atlantic atmosphere: links to primary productivity and nitrogen fixation. Deep-Sea Res. I54, 1704–1720.

Cape, J.N., Anderson, M., Rowland, A.P., Wilson, D., 2004. Organic nitrogen in precipitation across the United Kingdom. Water. Air. Soil. Pollut. Focus 4, 25–35.

Cape, J.N., Cornell, S.E., Jickells, T.D., Nemitz, E., 2011. Organic nitrogen in the atmosphere -Where does it come from? A review of sources and methods. Atmos. Res. 102, 30–48.

Carrillo, J.H., Hastings, M.G., Sigman, D.M., Huebert, B.J., 2002. Atmospheric deposition of inorganic and organic nitrogen and base cations in Hawaii. Glob. Biogeochem. Cy 16, 1076.

Chang, S.G., Novakov, T., 1975. Formation of pollution and particulate nitrogen compounds by NO-soot and NH_3-soot gas-particle surface reactions. Atmos. Environ. 9, 495–504.

Cornell, S.E., 2011. Atmospheric nitrogen deposition: revisiting the question of the importance of the organic component. Environ. Pollut. 159, 2214–2222.

Cornell, S.E., Jickells, T.D., Cape, J.N., Rowland, A.P., Duce, R.A., 2003. Organic nitrogen deposition on land and coastal environments: a review of methods and data. Atmos. Environ. 37, 2173–2191.

Cornell, S.E., Mace, K., Coeppicus, S., Duce, R., Huebert, B., Jickells, T., Zhuang, L.Z., 2001. Organic nitrogen in Hawaiian rain and aerosol. J. Geophys. Res. 106, 7973–7983.

Cornell, S.E., Rendell, A., Jickells, T., 1995. Atmospheric inputs of dissolved organic nitrogen to the oceans. Nature 376, 243–246.

Elliott, E.M., Kendall, C., Boyer, E.W., Burns, D.A., Lear, G., Golden, H.E., Harlin, K., Bytnerowicz, A., Butler, T.J., Glatz, R., 2009. Dual nitrate isotopes in actively and passively collected dry deposition: utility for partitioning NO_x sources contributing to landscape nitrogen deposition. J. Geophys. Res. 114, G04020.

Elliott, E.M., Kendall, C., Wankel, S.D., Burns, D., Boyer, E.W., Harlin, K., Bain, D., Butler, T.J., 2007. Nitrogen isotopes as indicators of NO_x source contributions to atmospheric nitrate deposition across the midwestern and northeastern United States. Environ. Sci. Technol. 41, 7661–7667.

Erbland, J., Vicars, W.C., Savarino, J., Morin, S., 2012. Air-snow transfer of nitrate on the East Antarctic Plateau – Part 1: isotopic evidence for a photolytically driven dynamic equilibrium. Atmos. Chem. Phys. 13 (13), 6403–6419.

Fang, Y.T., Koba, K., Wang, X.M., Wen, D.Z., Li, J., Takebayashi, Y., Liu, X.Y., Yoh, M., 2011. Anthropogenic imprints on nitrogen and oxygen isotopic composition of precipitation nitrate in a nitrogen-polluted city in Southern China. Atmos. Chem. Phys. 11, 1313–1325.

Felix, J.D., Elliott, E.M., Gish, T., Magrihang, R., Clougherty, J., Cambal, L., 2014. Examining the transport of ammonia emissions across landscapes using nitrogen isotope ratios. Atmos. Environ. 95, 563–570.

Felix, J.D., Elliott, E.M., Gish, T., McConnell, L., Shaw, S., 2013. Characterizing the isotopic composition of atmospheric ammonia emission sources using passive samplers and a combined oxidation-bacterial denitrifier isotope ratio mass spectrometer method. Rapid. Commun. Mass Sp. 27, 2239–2246.

Felix, J.D., Elliott, E.M., Shaw, S.L., 2012. The isotopic composition of coal-fired power plant NOx: the influence of emission controls and implications for global emission inventories. Environ. Sci. Technol. 46, 3528–3535.

Feuerstein, T.P., Ostrom, P.H., Ostrom, N.E., 1997. Isotopic biogeochemistry of dissolved organic nitrogen: a new technique and application. Org. Geochem 27, 363–370.

Fibiger, D.L., Hastings, M.G., 2016. First measurements of the nitrogen isotopic composition of NOx from biomass burning. Environ. Sci.Technol 50, 11569–11574.

Freyer, H.D., 1978. Seasonal trends of NH_4^+ and NO_3^- nitrogen isotope composition in rain collected at Jülich, Germany. Tellus 30, 83–92.

Freyer, H.D., 1991. Seasonal variation of $^{15}N/^{14}N$ ratios in atmospheric nitrate species. Tellus B 43, 30–44.

Freyer, H.D., Kley, D., Volz-Thomas, A., Kobel, K., 1993. On the interaction of isotopic exchange processes with photochemical reactions in atmospheric oxides of nitrogen. J. Geophys. Res. Atmos. 98 (D8), 14791–14796.

Geng, L., Alexander, B., Cole-Dai, J., Steig, E.J., Savarino, J., Sofen, E.D., Schauer, A.J., 2014. Nitrogen isotopes in ice core nitrate linked to anthropogenic atmospheric acidity change. Proc. Natl. Acad. Sci. U. S. A. 111 (16), 5808–5812.

Hastings, M.G., Jarvis, J.C., Steig, E.J., 2009. Anthropogenic impacts on nitrogen isotopes of ice-core nitrate. Science 324, 1288.

Hastings, M.G., Casciotti, K.L., Elliott, E.M., 2013. Stable isotopes as tracers of anthropogenic nitrogen sources, deposition, and impacts. Elements 9, 339–344.

Heaton, T.H.E., Spiro, B., Roberston, S.M.C., 1997. Potential canopy influences on the isotopic omposition of nitrogen and sulphur in atmospheric deposition. Oecologia 109, 600–660.

Heaton, T.H.E., 1987. $^{15}N/^{14}N$ ratio of nitrate and ammonium in rain of Pretoria, South Africa. Atmos. Environ. 21, 843–852.

Hoering, T., 1957. The isotopic composition of ammonia and the nitrate ion in rain. Geochim. Cosmochim. Acta 12, 97–102.

Kawashima, H., Kurahashi, T., 2011. Inorganic ion and nitrogen isotopic compositions of atmospheric aerosols at Yurihonjo, Japan: implications for nitrogen sources. Atmos. Environ. 45, 6309–6316.

Kendall, C., Elliott, E.M., Wankel, S.D., 2007. Tracing anthropogenic inputs of nitrogen to ecosystem. In: Lajtha, K., Michener, R.H. (Eds.), Stable Isotopes in Ecology and Environmental Science, second ed. Wiley–Blackwell Scientific Publication, pp. 375–449.

Knapp, A.N., Hastings, M.G., Sigman, D.M., Lipschultz, F., Galloway, J.N., 2010. The flux and isotopic composition of reduced and total nitrogen in Bermuda rain. Mar. Chem. 120, 83–89.

Knapp, A.N., Sigman, D.M., Lipschultz, F.N., 2005. Isotopic composition of dissolved organic nitrogen and nitrate at the Bermuda Atlantic time-series study site. Glob. Biogeochem. Cy. 19, GB1018.

Koba, K., Fang, Y.T., Mo, J.M., Zhang, W., Lu, X.K., Liu, L., Zhang, T., Takebayashi, Y., Toyoda, S., Yoshida, N., Suzuki, K., Yoh, M., Senoo, K., 2012. ^{15}N natural abundance of the N lost from an N-saturated subtropical forest in southern China. J. Geophys. Res. 117, G02015.

Koba, K., Inagaki, K., Sasaki, Y., Takebayashi, Y., Yoh, M., 2010. Nitrogen isotopic analysis of dissolved inorganic and organic nitrogen in soil extracts. In: Ohkouchi, N., Tayasu, I., Koba, K. (Eds.), Earth, Life and Isotopes. Kyoto University Press, pp. 17–37.

Li, D., Wang, X., 2008. Nitrogen isotopic signature of soil-released nitric oxide (NO) after fertilizer application. Atmos. Environ. 42, 4747–4754.

Li, J., Fang, Y.T., Yoh, M., Wang, X.M., Wu, Z.Y., Kuang, Y.W., Wen, D.Z., 2012. Organic nitrogen deposition in precipitation in metropolitan Guangzhou city of Southern China. Atmos. Res. 113, 57–67.

Liu, X.Y., Koba, K., Liu, C.Q., Li, X.D., Yoh, M., 2012. Pitfalls and new mechanisms in moss isotopic bio-monitoring of atmospheric nitrogen deposition. Environ. Sci.Technol 46, 12557–12566.

Liu, X.Y., Koba, K., Makabe, A., Li, X.,D., Yoh, M., Liu, C.Q., 2013. Ammonium first: natural mosses prefer atmospheric ammonium but vary utilization of dissolved organic nitrogen depending on habitat and nitrogen deposition. New Phytol. 199, 407–419.

Mariappan, S., Exner, M.E., Martin, G.E., Spalding, R.F., 2009. Variability of anaerobic

animal waste lagoon delta^{15}N source signatures. Environ. Forens. 10 (1), 18–25.
Michalski, G.T., Meixner, M., Fenn, L., Hernandez, A., Sirulnik, E., Allen, M., 2004. Tracing atmospheric nitrate deposition in a complex semiarid ecosystem using $\Delta^{17}O$. Environ. Sci. Technol. 38, 2175–2181.
Monse, E.U., Spindel, W., Stern, M.J., 1969. Analysis of isotope-effect calculations illustrated with exchange equilibria among oxynitrogen compounds. ACS Adv. Chem. Ser. 89, 148–184.
Morin, S., Savarino, J., Frey, M.M., Yan, N., Bekki, S., Bottenheim, J.W., Martins, J.M.F., 2008. Tracing the origin and fate of NO_x in the arctic atmosphere using stable isotopes in nitrate. Science 322, 730–732.
Morin, S., Savarino, J., Frey, M.M., Domine, F., Jacobi, H.W., Kaleschke, L., Martins, J.M.F., 2009. Comprehensive isotopic composition of atmospheric nitrate in the Atlantic Ocean boundary layer from 65°S to 79°N. J. Geophys. Res. 114, D05303.
Na, K., Song, C., Switzer, C., Cocker, D.R., 2007. Effect of ammonia on secondary organic aerosol formation from α-pinene ozonolysis in dry and humid conditions. Environ. Sci. Technol. 41, 6096–6102.
Neff, J.C., Holland, E.A., Dentener, F.J., McDowell, W.H., Russell, K.M., 2002. The origin, composition and rates of organic nitrogen deposition: a missing piece of the nitrogen cycle? Biogeochemistry 57/58, 99–136.
Nozière, B., Dziedzic, P., Córdova, A., 2009. Products and kinetics of the liquid-phase reaction of glyoxal catalyzed by ammonium ions (NH_4^+). J. Phys.Chem. 113, 231–237.
Prospero, J.M., Barrett, K., Church, T., Dentener, F., Duce, R.A., Galloway, J.N., Levy, H., Moody, J., Quinn, P., 1996. Atmospheric deposition of nutrients to the North Atlantic basin. Biogeochemistry 35, 27–73.
Rendell, A.R., Ottley, C.J., Jickells, T.D., Harrison, R.M., 1993. The atmospheric input of nitrogen species to the North Sea. Tellus 45B, 53–63.
Russell, K.M., Galloway, J.N., Macko, S.A., Scudlark, J.R., 1998. Sources of nitrogen in wet deposition to the Chesapeake Bay region. Atmos. Environ. 32, 2453–2465.
Shi, J., Gao, H., Qi, J., Zhang, J., Yao, X., 2010. Sources, compositions, and distributions of water-soluble organic nitrogen in aerosols over the China Sea. J. Geophys. Res. 115, D17303.
Walters, W.W., Goodwin, S.R., Michalski, G., 2015. The nitrogen stable isotope composition (^{15}N) of vehicle emitted NO_x. Environ. Sci. Technol. 49, 2278–2285.
Walters, W.W., Simonini, D.S., Michalski, G., 2016. Nitrogen isotope exchange between NO and NO_2 and its implications for $\delta^{15}N$ variations in tropospheric NO_x and atmospheric nitrate. Geophys. Res. Lett. 43, 440–448.
Xiao, H.W., Xiao, H.Y., Long, A.M., Wang, Y.L., 2012. Who controls the monthly variations of NH_4^+ nitrogen isotope composition in precipitation? Atmos. Environ. 54, 201–206.
Xiao, H.W., Xiao, H.Y., Long, A.M., Wang, Y.L., Liu, C.Q., 2013. Chemical composition and source apportionment of rainwater in Guiyang, SW China. J. Atmos. Chem. 70, 269–281.
Xiao, H.Y., Liu, C.Q., 2002. Sources of nitrogen and sulfur in wet deposition at Guiyang, Southwest China. Atmos. Environ. 36, 5121–5130.
Xiao, H.Y., Liu, C.Q., 2011. Estimates of dry and wet deposition using tissue N contents and ^{15}N natural abundance in epilithic mosses in atmospheric NH_y-dominated areas. J. Geophys. Res. 116.
Zhang, Y., Liu, X.J., Fangmeier, A., Goulding, K.W.T., Zhang, F.S., 2008. Nitrogen inputs and isotopes in precipitation in the North China Plain. Atmos. Environ. 42, 1436–1448.
Zhang, Y., Song, L., Liu, X.J., Li, W.Q., Lü, S.H., Zheng, L.X., Bai, Z.C., Cai, G.Y., Zhang, F.S., 2012. Atmospheric organic nitrogen deposition in China. Atmos. Environ. 46, 195–204.